High accuracy line positions of the ν_1 fundamental band of $^{14}N_2{}^{16}O$

Bidoor AlSaif , Marco Lamperti , Davide Gatti , Paolo Laporta , Martin Fermann , Aamir Farooq , Oleg Lyulin , Alain Campargue , Marco Marangoni

PII: S0022-4073(18)30058-X
DOI: 10.1016/j.jqsrt.2018.03.005
Reference: JQSRT 6020

To appear in: *Journal of Quantitative Spectroscopy & Radiative Transfer*

Received date: 30 January 2018
Revised date: 6 March 2018
Accepted date: 6 March 2018

Please cite this article as: Bidoor AlSaif , Marco Lamperti , Davide Gatti , Paolo Laporta , Martin Fermann , Aamir Farooq , Oleg Lyulin , Alain Campargue , Marco Marangoni , High accuracy line positions of the ν_1 fundamental band of $^{14}N_2{}^{16}O$, *Journal of Quantitative Spectroscopy & Radiative Transfer* (2018), doi: 10.1016/j.jqsrt.2018.03.005

Highlights

- The ν_1 band of N_2O is measured with an extended-cavity quantum cascade laser near 7.8 μm
- The spectrometer is frequency locked to a Tm:based frequency comb at 1.9 μm
- 70 lines are measured with an estimated systematic uncertainty of 60 kHz.
- Accurate spectroscopic constants of the 10^00 upper state are derived
- The *rms* of the fit of the line centers is $\approx 4.8\times10^{-6}$ cm^{-1} (144 kHz)

High accuracy line positions of the ν_1 fundamental band of $^{14}N_2{}^{16}O$

Bidoor AlSaif[1], Marco Lamperti[2], Davide Gatti[2], Paolo Laporta[2], Martin Fermann[3], Aamir Farooq[1], Oleg Lyulin[4], Alain Campargue[5*], Marco Marangoni[2]

[1]*King Abdullah University of Science and Technology (KAUST), Clean Combustion Research Center (CCRC), Thuwal 23955, Saudi Arabia*

[2]*Physics Department of Politecnico di Milano and IFN-CNR, Via G. Previati 1/C, 23900 Lecco, Italy*

[3] *IMRA America Inc., 1044 Woodridge Avenue, Ann Arbor, MI 48105-9774, USA*

[4]*Laboratory of Theoretical Spectroscopy, V.E. Zuev Institute of Atmospheric Optics SB RAS, 1, Academician Zuev square, Tomsk 634021, Russia*

[5]*Univ. Grenoble Alpes, CNRS, LIPhy, 38000 Grenoble, France*

Number of pages: 15

Number of tables: 3

Number of figures: 3

Keywords: Nitrous oxide; Microwave, Mid-Infrared, Line position, Frequency comb, Quantum cascade laser

* Corresponding author
Tel: +33 4 76 51 43 19
E-mail address: Alain.Campargue@univ-grenoble-alpes.fr

Abstract

The ν_1 fundamental band of N_2O is examined by a novel spectrometer that relies on the frequency locking of an external-cavity quantum cascade laser around 7.8 μm to a near-infrared Tm:based frequency comb at 1.9 μm. Due to the large tunability, nearly 70 lines in the 1240 – 1310 cm^{-1} range of the ν_1 band of N_2O, from *P*(40) to *R*(31), are for the first time measured with an absolute frequency calibration and an uncertainty from 62 to 180 kHz , depending on the line. Accurate values of the spectroscopic constants of the upper state are derived from a fit of the line centers (*rms* ≈ 4.8×10^{-6} cm^{-1} or 144 kHz). The ν_1 transitions presently measured in a Doppler regime validate high accuracy predictions based on sub-Doppler measurements of the ν_3 and ν_3-ν_1 transitions.

1. Introduction

Even in their most recent editions [1], line parameters included in spectroscopic databases relies on absorption spectra measured by Fourier Transform Spectroscopy (FTS). This approach limits traceability and accuracy of line positions to a few tens of MHz, which explains why most lines, even those from the more intense bands, are usually given with a 10^{-4} – 10^{-3} cm^{-1} (3–30 MHz) uncertainty. The invention of optical frequency combs at the end of the past millennium enabled the calibration of optical frequencies against primary frequency standards, whose fractional frequency uncertainty may easily attain ~ 10^{-11} at 1 s. This made it possible, at least on single transitions, to retrieve line centers with uncertainties down to a few kHz [2–7].

On the other hand, optical frequency combs have been seldom applied to broad line surveys to extract spectroscopic parameters of molecular absorption bands. In the near-infrared (near-IR), extended measurements have been performed only on a few bands of C_2H_2, NH_3 and H_2O in a sub-Doppler regime [6–10] and of CO, CO_2 and H_2O in a Doppler broadening regime [11–15], quite often in conjunction with optical cavities to extend the effective absorption path length (as well as to enhance the laser intensity in saturated surveys). In the mid-IR, surveys over more than 50 cm^{-1} have been provided for the ν_3 band of N_2O [16] and of CH_4 [17,18], as well as for CO_2 near 4.3 and 2.7 μm [19,20]. A technological hurdle here originating from the lack of commercial mid-IR comb synthesizers and hence from the need to resort to nonlinear optics to get referencing of a mid-IR probe laser to a near-IR comb [21–28]. A second nontrivial requirement is a widely tunable single-mode laser, most of all beyond 5 μm, where cw sources based on difference-frequency-generation or optical parametric oscillation are not available. Distributed-feedback (DFB) quantum cascade lasers are an option only for rather narrow ranges of about 10 cm^{-1} [29], whereas for ranges of ~100 cm^{-1}, which are needed to cover an entire absorption band, the only solution available commercially is given by external cavity quantum cascade lasers (EC-QCLs). As these lasers usually suffer from a large amount of frequency noise [30], their use in combination with frequency combs has been firstly demonstrated in an unlocked regime, with an accuracy of 800 kHz [31], and only recently in a comb-locked regime with an accuracy of 60 kHz [32].

In this work, the spectrometer proposed in Ref. [32] is applied to the first high accuracy line position measurements of the ν_1 fundamental band of $^{14}N_2{}^{16}O$ near 1285 cm^{-1}. The measured positions are used to derive spectroscopic parameters of the upper state. Specifically, nearly 70 lines equally distributed among the P and R branches have been measured with a systematic uncertainty of 60 kHz and a statistical uncertainty varying from 10 to 170 kHz depending on the line. It is worth noting that the impact of the statistical uncertainty on the spectroscopic parameters is strongly reduced by the averaging effect that takes place when all lines are considered in a global fitting procedure, this being one of the major strengths of the broadband comb-calibrated approach described herein.

2. Experimental

The spectrometer is described in detail in Ref. [32]. It is based on the frequency locking of an external cavity quantum cascade laser (EC-QCL) from Daylight Solutions, with tunability from 7.55 to 8.2 μm and optical power above 60 mW after optical isolation, to a Tm:fiber frequency comb at 1.9 μm delivering up to 1.5 W at a repetition rate of 100 MHz [33]. The layout of the spectrometer is depicted in **Fig. 1**. The referencing scheme relies on a sum frequency generation (SFG) process [26,34] between the comb and the EC-QCL in an 8-mm-long Zinc-Germanium Phosphide (ZGP) crystal: this process generates a new comb (ν_{SFG}) near 1.54 μm whose frequency is offset from the original comb (ν_m) by the EC-QCL frequency (ν_{QCL}), i.e., $\nu_{SFG} = \nu_m + \nu_{QCL}$. Thereafter, by heterodyning the SFG comb against a spectrally broadened replica of the original near-IR comb (ν_n), a radio-frequency (RF) beat note (f_{beat}) is extracted, $f_{beat} = |\nu_{SFG} - \nu_n| = |\nu_{QCL} - (n-m) f_{rep}|$, which allows the EC-QCL frequency to be calibrated against an integer multiple ($n-m$) of the comb repetition frequency (f_{rep}). The stabilization of f_{beat} against an RF local oscillator (f_{LO}) is obtained by driving the EC-QCL piezo modulation port with a servo PID. By scanning the repetition rate of the frequency comb while maintaining a steady frequency lock of EC-QCL to the comb ($f_{beat} = f_{LO}$), one can finely tune the EC-QCL over ~ 600 MHz. The absolute frequency calibration derives from the fact that all radiofrequencies, namely f_{rep} and f_{LO}, and hence all optical frequencies are seeded by a primary clock based on a GPS-disciplined Rb oscillator. As compared to the setup described in Ref. [32], an intensity stabilization scheme was added to compensate for laser fluctuations during the spectral scans and thus to achieve a flatter

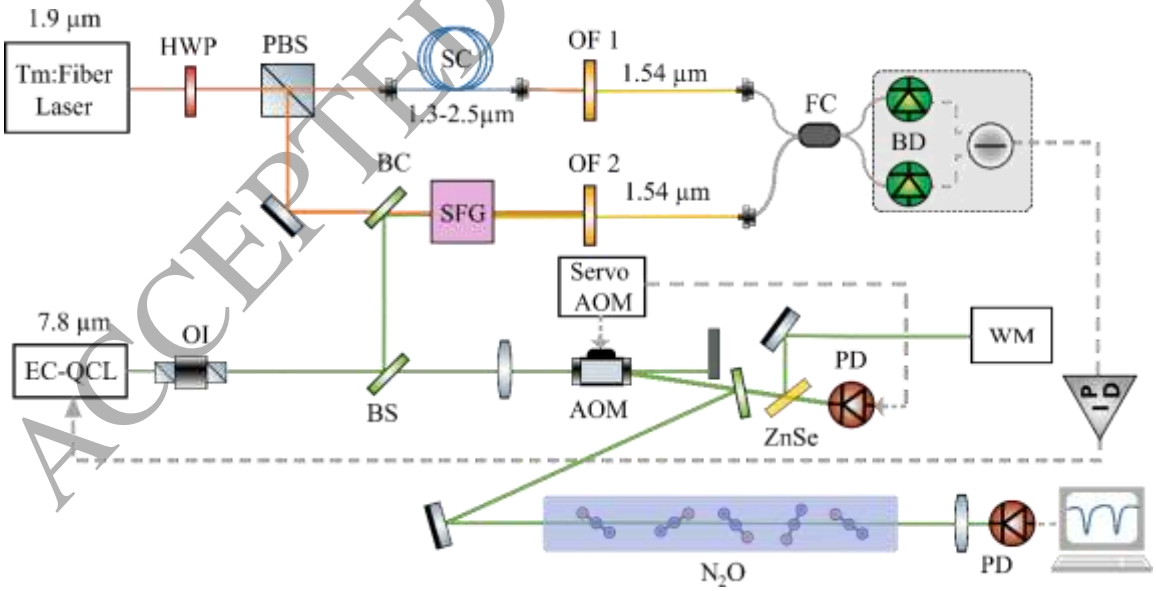

Fig. 1: Layout of the spectrometer, based on the frequency locking of a mid-IR EC-QCL to a near-IR Tm frequency comb. HWP: half wave plate, PBS: polarizing beam splitter, SC: supercontinuum, BS: beam splitter, BC: beam combiner, PD: photodetector, OF: optical filter, FC: fiber coupler, BD: balanced detector, SFG: Sum-Frequency-Generation, OI: optical isolator, AOM: acousto-optic modulator, and WM: wavemeter.

baseline. This was obtained by introducing an acousto-optic modulator in the beam path and by actively controlling its input RF power in such a way as to keep the diffracted field power stable around a 0.5 mW set-point. A photodetector placed upstream the optical cell serves as a monitor for the intensity stabilization feedback loop.

In this work, we fully exploit the wide tunability and the single-mode operation of the EC-QCL to cover 70 absorption lines of nitrous oxide (N_2O) spanning the 1240 – 1310 cm^{-1} range. The gas is housed in a 66 cm long optical cell kept at room temperature and at pressures of 0.01 – 0.04 mbar (1 – 4 Pa), in a regime where absorption profiles are almost exclusively determined by Doppler broadening and self-induced pressure shift of the line center is negligible. The measurements are performed by a fully automated setup that reads the EC-QCL frequency out of a wavemeter (WM), tunes it to the target absorption line, switches on the lock to the frequency comb, steps the comb repetition rate by 4 Hz (1.5 MHz in the optical domain) to scan and acquire the absorption line, switches off the lock, then again tunes the laser frequency to the next line of a preliminarily uploaded HITRAN list. Typically, a 540 MHz-wide spectrum consists of 360 evenly spaced points acquired with a

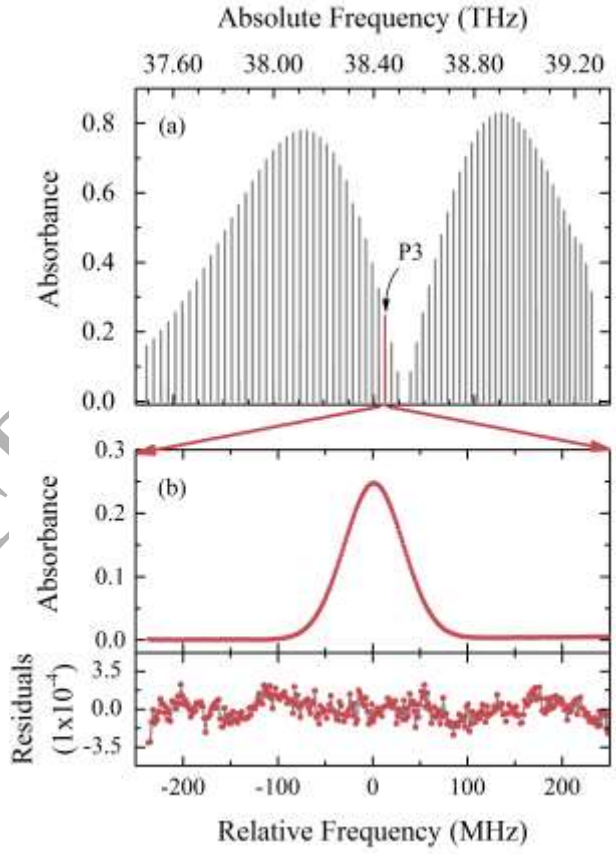

Fig. 2: (a) Absorption spectrum of the ν_1 band of N_2O at room temperature and at a 0.018 mbar pressure. (b) zoomed-in view of the P(3) line together with residuals from a Gaussian fitting.

dwell time of 100 ms.

An overview of the measurements of the ν_1 band of N_2O is presented in **Fig. 2** (a). The absorption spectra cover most part of the *P* and *R* lines up to $J = 40$ and $J = 31$, respectively. Each line results from the average of 10 spectra acquired in 6 minutes. To maintain an almost uniform signal-to-noise ratio for lines with different strengths, the acquisition has been split in separated runs at slightly different pressures, from 0.01 to 0.04 mbar (for representation purposes, the experimental absorbance values have been normalized in **Fig. 2** to the same pressure condition of 0.018 mbar). Such low-pressure regime allowed us to fit the absorption lines with a Gaussian profile. As a representative case, **Fig. 2** (b) reports a 10-times averaged spectrum of the *P*(3) line together with the residuals obtained from a fitting that includes a linear slope for the baseline: the latter are only slightly affected by parasitic etalons and laser intensity noise. The signal-to-noise ratio is about 890.

Uncertainty source	Type A (kHz)	Type B (kHz)
Experimental reproducibility	10 – 170 kHz	
Frequency scale uncertainty		0.5
Pressure reading & leakage		1
Pressure shift calibration		2
Laser lineshape asymmetry		60
Total uncertainty	62 – 180 kHz	

Table 1. Uncertainty budget for the individual line center.

The statistical uncertainty (Type A error calculated as the standard error of the mean) on the line centers varies, depending on the line, from 10 kHz to 170 kHz. These numbers reflect the noise level on the vertical axis of the measurement, some nonlinearity of the spectral baseline and also the stability of the laser frequency. The sources of systematic uncertainty (Type B error) are quantified and detailed in **Table 1**. Minor contributions come from the stability of the GPS frequency standard (~ 0.5 kHz over a 6 minute long measurement), from the uncertainty of the absolute pressure gauge used in the experiments (10 %) and from the cell leakage (0.0065 mbar/h): the latter two terms, as weighted by pressure shift coefficients of the order of -26 kHz/mbar, contribute to an uncertainty of about 1 kHz. Those coefficients have been taken from HITRAN [1], and refer to an air mixture instead of a pure sample, but as the pressure adopted herein is very low, this does not affect the accuracy budget by more than 2 kHz. The major systematic limitation is ascribed to an asymmetric shape of the laser emission (see details in Ref.[32]), which we accounted for by recording, during each spectral scan, the electrical spectrum of the beatnote between the laser and comb, then by deconvolving every absorption profile by the laser emission line. In the error budget table, the 60 kHz uncertainty assigned to the laser line shape corresponds to the *rms* value of a distribution of line centers (of a single transition) acquired in different conditions, either reversing the sign of the frequency lock or changing the local oscillator frequency. The quadrature addition of Type A and Type B errors returns global uncertainty ranging from 62

to 180 kHz depending on the line. The ν_1 line positions with their corresponding experimental errors are listed in **Table 2.**

3. Line position analysis

3.1 Spectroscopic parameters

The set of measured transition frequencies was used to derive the parameters of the 10^00 upper vibrational state through the standard expression for rovibrational energy levels:

$$F_v(J)= G_v +B_vJ(J+1)-D_vJ^2(J+1)^2+H_vJ^3(J+1)^3+ L_vJ^4(J+1)^4 \quad (1)$$

where G_v is the vibrational term value, B_v is the rotational constant, D_v, H_v and L_v are centrifugal distortion constants, and J is the angular momentum quantum number. The ground state (GS) constants were constrained to the accurate values reported by Ting et al. [16]. These GS constants were obtained from a global fit involving different sets of highly accurate measurements including fourteen line center values of GS rotational transitions with accuracy better than 1 kHz. Here, after excluding six weak *P(J)* lines with *J* values between 29 and 43 measured with lower accuracy, an *rms* deviation of 4.8×10^{-6} cm^{-1} (144 kHz) is achieved for 66 line positions covering the *P*(40) – *R*(31) range. This *rms* value is consistent with the error budget described in **Table 1**. The obtained spectroscopic constants are listed in **Table 3** together with the GS constants of Ref. [16]. Differences of measured and calculated line positions are displayed in **Fig. 3** and listed in **Table 2** together with the corresponding calculated GS energy levels and ν_1 line position values for all transitions up to J_{up}= 45.

3.2 Comparison to literature

The HITRAN2016 database [1] reproduces the ν_1 line positions calculated using the spectroscopic parameters (SP) given by Toth on his website [35] (see **Table 3)**. By using long absorption path lengths (up to 70 m), Toth could detect high *J* rotational lines up to *P*(86) and *R(*89) which are listed in Ref. [35]. Toth's line list, as reproduced in HITRAN, covers the *P*(87) – *R(*87) range of transitions. H_v and L_v distortion terms were needed to reproduce the measured dataset. In Ref. [35],Toth did not provide line position uncertainties or error bars on his band parameters. The deviations of HITRAN values to our fitted values are plotted in **Fig. 3** together with the deviations of Toth's original measurements [35]. Compared to HITRAN, deviations up to 6×10^{-5} cm^{-1} (1.8 MHz) are observed in the range of our observations. These values are fully consistent with the uniform HITRAN error bar ($<10^{-3}$ cm^{-1}) attached to the ν_1 line positions.

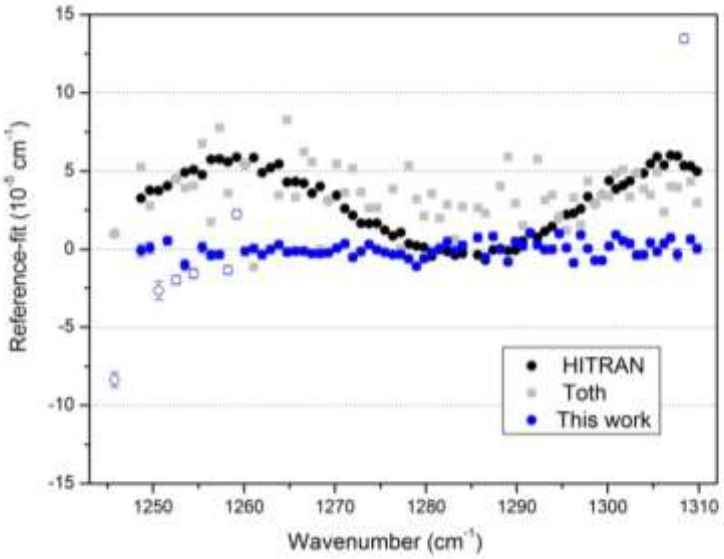

Fig. 3. Deviations from the fitted position values of the ν_1 fundamental band of $^{14}N_2{}^{16}O$ of *(i)* the experimental values measured in this work (full blue circles; open circles correspond to transitions excluded from the fit), *(ii)* the HITRAN2016 values [1] (full black circles) and *(iii)* the original measurements by Toth [35] (grey squares).

An exhaustive literature review (up to 2012) of the $^{14}N_2{}^{16}O$ line position measurements from 0 to 10000 cm^{-1} can be found in Table 2 of Ref. [36], which includes estimated values for the precision of each experimental source. According to this review, a number of studies have reported positions of pure $R(J)$ rotational lines with accuracy of ~ tens of kHz in both the ground [37–40] and 10^00 excited states [37,38,41,42]. The 10^00 upper state of the ν_1 band is also involved in sub-Doppler frequency measurements of the (ν_3–ν_1) band near 9 µm performed by Tachikawa et al. [14] by using a heterodyne difference frequency technique with fluorescence-stabilized CO_2 lasers. The (ν_3-ν_1) transition frequencies of the $P(38)$ – $R(18)$ lines were reported with an accuracy better than 5 kHz for most of the lines and the authors combined their results with literature measurements (including Toth's measurements) to derive effective spectroscopic parameters (SP) for the 10^00, 00^01, 02^00 and 02^20 states. The derived SPs of the 10^00 state considered as an isolated state (as in our analysis) are included in **Table 3**. The most significant difference concerns the vibrational term which was reported with a 107 kHz and 750 kHz relative and absolute 1σ uncertainty, respectively [14]. Our vibrational term value obtained from the direct measurement of the ν_1 band transitions is determined with a 36 kHz and 100 kHz relative and absolute uncertainty and differs by about 920 kHz compared to Ref. [14].

As mentioned above, the results recently reported by Ting et al. [16] in sub-Doppler regime have supplanted most of the previous studies in terms of accuracy of rotational transitions in N_2O. By locking their synthesizer to a cesium clock, they determined the frequency of 175 pure rotational transitions within five vibrational states (including the 10^00 state). Overall, 33 values with sub-Doppler precision (0.5 – 3 kHz) and 142 with Doppler limited precision were reported. In addition, using a difference frequency generation (DFG) source calibrated by an optical frequency comb, Ting et al. determined 44 saturated absorption line centers of the ν_3 band near 2223 cm^{-1}, with an accuracy better than 10 kHz for most transitions [16]. Using their sets of microwave and infrared data with *J* up to 100 and combined with literature precision measurements (in particular those by Tachikawa et al. [14]), Ting et al. developed an effective Hamiltonian (EH) model to reproduce the transition frequencies involving the 00^00, 01^10, 10^00, 00^01, 02^00 and $02^{\pm2}0$ interacting states. An overall ensemble of 860 selected transitions was used to fit the model parameters and predictions were obtained for the pure rotational band and for the fundamental bands, including the ν_1 band of present interest. The combination of the ν_3 measurements by Ting et al. with those of Tachikawa et al. for the (ν_3-ν_1) band, both with accuracy at the kHz level, allows for very accurate predictions of the frequency of the ν_1 transitions. The resulting calculated line list was not provided in the Supplemental Material of Ref. [16] but can be found in the JPL spectral line catalog [43]. In the range of our measurements, the ν_1 band predicted frequencies are provided with a typical accuracy of 3 kHz. The average and *rms* of the differences between the position values computed from our ν_1 band spectroscopic parameters and those predicted in Ref. [16] are -72 and 54 kHz, respectively, then fully consistent with our claimed error bars (**Table 1**).

4. Conclusion

The transition frequencies of 72 lines of the ν_1 fundamental band of $^{14}N_2{}^{16}O_2$ have been for the first time directly measured with high accuracy by a novel spectrometer that relies on the frequency locking of an EC-QCL around 7.8 μm to a Tm:based frequency comb at 1.9 μm. Line centers are reported with an uncertainty ranging between 62 and 180 kHz. Using an isolated band model, line positions were reproduced with an *rms* of 144 kHz allowing for an accurate determination of the spectroscopic parameters of the 10^00 level. Compared to the HITRAN line list of N_2O, based on FTS measurements by Toth [35,44], significant deviations are evidenced but their amplitude is largely below the HITRAN error bar ($<10^{-3}$ cm^{-1}).

Because of the approximate $\omega_3 \cong 2\omega_1 \cong 4\omega_2$ relations between harmonic frequencies, the $^{14}N_2{}^{16}O$ vibrational states are involved in a set of couplings that need a global modeling [36]. Using such an effective Hamiltonian model, Ting et al. reproduced a large set of sub-Doppler precision measurements involving the ground and first vibrational states [16]. For the ν_1 band our data provide a validation of these predictions within 72 kHz, which is consistent with our 1σ uncertainty. This prompts the incorporation of Ting's data into future versions of spectroscopic databases.

Table 2.

Measured and calculated values of the line positions of the ν_1 band of $^{14}N_2{}^{16}O$ and corresponding deviations.

Transition	Measured (cm^{-1})	Calculated (cm^{-1})	Meas.- Calc.[a] (10^{-5} cm^{-1})	Ground state [b] (cm^{-1})
P46		1242.8044486		905.0784946
P45		1243.7946864		866.5980671
P44		1244.7817034		828.9512843
P43	1245.7654065(47)	1245.7654902	-8.37*	792.1383367
P42		1246.7460375		756.1594102
P41		1247.7233362		721.0146869
P40	1248.6973766(38)	1248.6973774	-0.08	686.7043444
P39	1249.6681532(36)	1249.6681523	0.09	653.2285561
P38	1250.6356260(61)	1250.6356525	-2.65*	620.5874912
P37	1251.5998748(28)	1251.5998694	0.54	588.7813147
P36	1252.5607752(29)	1252.5607949	-1.97*	557.8101873
P35	1253.5184108(34)	1253.5184208	-1.00	527.6742655
P34	1254.4727237(31)	1254.4727393	-1.55*	498.3737015
P33	1255.4237436(33)	1255.4237424	0.12	469.9086434
P32	1256.3714189(32)	1256.3714226	-0.37	442.2792348
P31	1257.3157688(24)	1257.3157723	-0.35	415.4856155
P30	1258.2567709(25)	1258.2567842	-1.34*	389.5279206
P29	1259.1944735(27)	1259.1944511	2.24*	364.4062813
P28	1260.1287645(26)	1260.1287658	-0.13	340.1208244
P27	1261.0597220(25)	1261.0597214	0.05	316.6716725
P26	1261.9873075(26)	1261.9873110	-0.35	294.0589441
P25	1262.9115278(26)	1262.9115279	-0.01	272.2827532
P24	1263.8323685(25)	1263.8323655	0.30	251.3432098
P23	1264.7498155(26)	1264.7498172	-0.17	231.2404196
P22	1265.6638756(24)	1265.6638767	-0.12	211.9744841
P21	1266.5745366(26)	1266.5745378	-0.12	193.5455005
P20	1267.4817915(25)	1267.4817942	-0.27	175.9535618
P19	1268.3856371(24)	1268.3856399	-0.28	159.1987567
P18	1269.2860668(24)	1269.2860690	-0.22	143.2811699
P17	1270.1830762(24)	1270.1830756	0.07	128.2008816
P16	1271.0766575(24)	1271.0766539	0.36	113.9579679
P15	1271.9667933(24)	1271.9667984	-0.51	100.5525007
P14	1272.8535020(24)	1272.8535034	-0.14	87.9845476
P13	1273.7367667(24)	1273.7367636	0.31	76.2541721
P12	1274.6165732(24)	1274.6165734	-0.02	65.3614332
P11	1275.4929258(24)	1275.4929278	-0.20	55.3063860
P10	1276.3658180(24)	1276.3658215	-0.35	46.0890812
P9	1277.2352460(24)	1277.2352494	-0.33	37.7095653
P8	1278.1012004(24)	1278.1012065	-0.61	30.1678805
P7	1278.9636770(24)	1278.9636879	-1.09	23.4640648
P6	1279.8226829(24)	1279.8226888	-0.59	17.5981522
P5	1280.6782025(25)	1280.6782044	-0.20	12.5701721
P4	1281.5302307(26)	1281.5302302	0.06	8.3801499
P3	1282.3787661(32)	1282.3787614	0.46	5.0281069
P2	1283.2237929(26)	1283.2237938	-0.09	2.5140598
P1	1284.0653252(27)	1284.0653228	0.25	0.8380213
R0	1285.7378611(27)	1285.7378536	0.75	0
R1	1286.5688416(25)	1286.5688470	-0.53	0.8380213
R2	1287.3963286(26)	1287.3963203	0.82	2.5140598
R3	1288.2202697(25)	1288.2202696	0.00	5.0281069
R4	1289.0406830(24)	1289.0406910	-0.80	8.3801499
R5	1289.8575856(25)	1289.8575806	0.50	12.5701721
R6	1290.6709368(24)	1290.6709348	0.20	17.5981522
R7	1291.4807603(24)	1291.4807498	1.05	23.4640648
R8	1292.2870252(24)	1292.2870223	0.29	30.1678805
R9	1293.0897483(25)	1293.0897486	-0.03	37.7095653
R10	1293.8889255(24)	1293.8889255	0.00	46.0890812
R11	1294.6845596(24)	1294.6845496	1.00	55.3063860
R12	1295.4766188(24)	1295.4766178	0.10	65.3614332
R13	1296.2651184(24)	1296.2651270	-0.86	76.2541721
R14	1297.0500833(24)	1297.0500742	0.91	87.9845476
R15	1297.8314570(24)	1297.8314564	0.05	100.5525007
R16	1298.6092638(24)	1298.6092710	-0.72	113.9579679
R17	1299.3835079(24)	1299.3835150	-0.72	128.2008816
R18	1300.1541880(24)	1300.1541861	0.20	143.2811699
R19	1300.9212906(25)	1300.9212816	0.91	159.1987567
R20	1301.6848044(24)	1301.6847991	0.53	175.9535618
R21	1302.4447399(27)	1302.4447363	0.36	193.5455005
R22	1303.2010874(26)	1303.2010912	-0.38	211.9744841
R23	1303.9538578(27)	1303.9538615	-0.36	231.2404196

R24	1304.7030494(26)	1304.7030453	0.41	251.3432098
R25	1305.4486393(25)	1305.4486407	-0.14	272.2827532
R26	1306.1906499(26)	1306.1906462	0.37	294.0589441
R27	1306.9290673(25)	1306.9290599	0.74	316.6716725
R28	1307.6638771(37)	1307.6638805	-0.34	340.1208244
R29	1308.3949719(26)	1308.3951065	13.47*	364.4062813
R30	1309.1227432(27)	1309.1227368	0.64	389.5279206
R31	1309.8467707(29)	1309.8467703	0.04	415.4856155
R32		1310.5672059		442.2792348
R33		1311.2840430		469.9086434
R34		1311.9972807		498.3737015
R35		1312.7069187		527.6742655
R36		1313.4129564		557.8101873
R37		1314.1153937		588.7813147
R38		1314.8142305		620.5874912
R39		1315.5094670		653.2285561
R40		1316.2011033		686.7043444
R41		1316.8891399		721.0146869
R42		1317.5735775		756.1594102
R43		1318.2544168		792.1383367
R44		1318.9316588		828.9512843

Notes

[a] Values with asterisk (*) were excluded from the fit.

[b] The ground state energy levels given in the last column were calculated using the parameters values reported by Ting et al. [16].

Table 3.

Spectroscopic parameters (in cm^{-1}) of the ground and (10^00) upper vibrational states of $^{14}N_2{}^{16}O$ derived from the ν_1 line positions measured between 1248 and 1310 cm^{-1} using a comb-locked extended-cavity quantum-cascade-laser, together with a comparison with literature.

$V_1V_2\ell_2V_3$	G_v	B_v	$D_v\times10^6$	$H_v\times10^{12}$	$L_v\times10^{18}$	*observed lines*	*RMS*[a]	*Ref.*
00^00	0.0	0.419011001(20)	0.17609193(3042)	-0.016529(2400)	0			Toth [35,44].
10^00	1284.90334	0.417255210	0.1726978	0.14666	1.853	*P*(87)-*R*(87)		Toth [44]
00^00	0.0	0.41901101941	0.176106765	-0.015547	-0.308			Ting et al. [16]
10^00	1284.9033344(13)	0.417255073(10)	0.172597(18)	0.1307(86)		*P*(43)-*R*(31)	4.3×10^{-6}	This work
10^00	1284.9033624(36) [b]	0.4172550738 (14)	0.172768(13)	0.1164(46)		*P*(38)-*R*(18)		Tachikawa et al. [14]

Notes

The uncertainties (1σ) are given in parenthesis in the unit of the last quoted digit.

[a] Root Mean Square of the (Meas.-Calc.) differences of the position values

[b] The absolute (1σ) uncertainties are 100 kHz and 750 kHz (3.3×10^{-6} and 2.5×10^{-5} cm^{-1}) for this work and Ref. [14], respectively.

References:

[1] Gordon IE, Rothman LS, Hill C, Kochanov RV, Tan Y, Bernath PF, et al. The HITRAN2016 molecular spectroscopic database. J Quant Spectrosc Radiat Transf 2017;203:3–69. doi:10.1016/J.JQSRT.2017.06.038.

[2] Holzwarth R, Nevsky AY, Zimmermann M, Udem T, Hänsch TW, von Zanthier J, et al. Absolute frequency measurement of iodine lines with a femtosecond optical synthesizer. Appl Phys B 2001;73:269–71. doi:10.1007/s003400100633.

[3] Hong F-L, Onae A, Jiang J, Guo R, Inaba H, Minoshima K, et al. Absolute frequency measurement of an acetylene-stabilized laser at 1542 nm. Opt Lett 2003;28:2324. doi:10.1364/OL.28.002324.

[4] Amy-Klein A, Goncharov A, Daussy C, Grain C, Lopez O, Santarelli G, et al. Absolute frequency measurement in the 28 THz spectral region with a femtosecond laser comb and a long-distance optical link to a primary standard. Appl Phys B Lasers Opt 2004;78:25–30. doi:10.1007/s00340-003-1335-z.

[5] Mazzotti D, Cancio P, Giusfredi G, De Natale P, Prevedelli M. Frequency-comb-based absolute frequency measurements in the mid-infrared with a difference-frequency spectrometer. Opt Lett 2005;30:997–9. doi:10.1364/OL.30.000997.

[6] Edwards CS, Barwood GP, Margolis HS, Gill P, Rowley WRC. High-precision frequency measurements of the $\nu_1+\nu_3$ combination band of $^{12}C_2H_2$ in the 1.5μm region. J Mol Spectrosc 2005;234:143–8. doi:10.1016/j.jms.2005.08.014.

[7] Madej AA, Bernard JE, John Alcock A, Czajkowski A, Chepurov S. Accurate absolute frequencies of the $\nu_1+\nu_3$ band of $^{13}C_2H_2$ determined using an infrared mode-locked Cr:YAG laser frequency comb. J Opt Soc Am B 2006;23:741. doi:10.1364/JOSAB.23.000741.

[8] Twagirayezu S, Cich MJ, Sears TJ, McRaven CP, Hall GE. Frequency-comb referenced spectroscopy of ν_4- and ν_5-excited hot bands in the 1.5μm spectrum of C_2H_2. J Mol Spectrosc 2015;316:64–71. doi:10.1016/j.jms.2015.06.010.

[9] Czajkowski A, Alcock AJ, Bernard JE, Madej AA, Corrigan M, Chepurov S. Studies of saturated absorption and measurements of optical frequency for lines in the $\nu_1 + \nu_3$ and $\nu_1 + 2\nu_4$ bands of ammonia at 1.5 μm. Opt Express 2009;17:9258. doi:10.1364/OE.17.009258.

[10] Gambetta A, Fasci E, Castrillo A, Marangoni M, Galzerano G, Casa G, et al. Frequency metrology in the near-infrared spectrum of $H_2{}^{17}O$ and $H_2{}^{18}O$ molecules: Testing a new inversion method for retrieval of energy levels. New J Phys 2010;12:103006. doi:10.1088/1367-2630/12/10/103006.

[11] Mondelain D, Sala T, Kassi S, Romanini D, Marangoni M, Campargue A. Broadband and highly sensitive comb-assisted cavity ring down spectroscopy of CO near 1.57μm with sub-MHz frequency accuracy. J Quant Spectrosc Radiat Transf 2015;154:35–43. doi:10.1016/j.jqsrt.2014.11.021.

[12] Long DA, Wójtewicz S, Miller CE, Hodges JT. Frequency-agile, rapid scanning cavity ring-down spectroscopy (FARS-CRDS) measurements of the (30012)←(00001) near-infrared carbon dioxide band. J Quant Spectrosc Radiat Transf 2015;161:35–40. doi:10.1016/j.jqsrt.2015.03.031.

[13] Mondelain D, Mikhailenko SN, Karlovets EV, Béguier S, Kassi S, Campargue A. Comb-assisted cavity ring down spectroscopy of ^{17}O enriched water between 7443 and 7921 cm^{-1}. J

Quant Spectrosc Radiat Transf 2017;203:206–12. doi:10.1016/j.jqsrt.2017.03.029.

[14] M. Tachikawa, K. M. Evenson, L. R. Zink, A. G. Maki. Frequency Measurements of 9 and 10 μm N2O Laser Transitions. IEEE J Quantum Electron 1996;32:1732–6. doi:10.1109/3.538777.

[15] Mikhailenko SN, Mondelain D, Karlovets E V., Kassi S, Campargue A. Comb-Assisted Cavity Ring Down Spectroscopy of ^{17}O enriched water between 6667 and 7443 cm^{-1}. J Quant Spectrosc Radiat Transf 2018;206:163–71. doi:10.1016/j.jqsrt.2017.10.023.

[16] Ting W-J, Chang C-H, Chen S-E, Chen H-C, Shy J-T, Drouin BJ, et al. Precision frequency measurement of N_2O transitions near 4.5 μm and above 1.50 μm. J Opt Soc Am B 2014;31:1954. doi:10.1364/JOSAB.31.001954.

[17] Okubo S, Nakayama H, Iwakuni K, Inaba H, Sasada H. Absolute frequency list of the ν3-band transitions of methane at a relative uncertainty level of 10^{-11}. Opt Express 2011;19:23878–88.

[18] Baumann E, Giorgetta FR, Swann WC, Zolot AM, Coddington I, Newbury NR. Spectroscopy of the methane ν_3 band with an accurate midinfrared coherent dual-comb spectrometer. Phys Rev A 2011;84:62513. doi:10.1103/PhysRevA.84.062513.

[19] Liao C-C, Wu K-Y, Lien Y-H, Shy J-T, Chou C-C. High precision MID-IR spectroscopy of of $^{12}C_{16}O_2$: 00^01. Int Symp Mol Spectrosc 2008;Paper FA09.

[20] Guan Y-C, Patel DN, Peng B-H, Suen T-H, Wang L-B, Shy J-T. Frequency measurements and molecular constants of the $^{12}C^{16}O_2$ $[10^01, 02^01]_{II} \leftarrow 00^00$ band near 2.7 μm. J Mol Spectrosc 2017;334:26–30. doi:10.1016/J.JMS.2017.03.011.

[21] Foreman SM, Marian A, Ye J, Petrukhin E a, Gubin M a, Mücke OD, et al. Demonstration of a HeNe/CH_4-based optical molecular clock. Opt Lett 2005;30:570–2. doi:10.1364/OL.30.000570.

[22] Gambetta A, Cassinerio M, Coluccelli N, Fasci E, Castrillo A, Gianfrani L, et al. Direct phase-locking of a 8.6μm quantum cascade laser to a mid-IR optical frequency comb: application to precision spectroscopy of N2O. Opt Lett 2015;40:304. doi:10.1364/OL.40.000304.

[23] Adler F, Cossel KC, Thorpe MJ, Hartl I, Fermann ME, Ye J. Phase-stabilized, 1.5 W frequency comb at 2.8–4.8 μm. Opt Lett 2009;34:1330–2. doi:10.1364/OL.34.001330.

[24] Amy-Klein A, Goncharov A, Guinet M, Daussy C, Lopez O, Shelkovnikov A, et al. Absolute frequency measurement of a SF_6 two-photon line by use of a femtosecond optical comb and sum-frequency generation. Opt Lett 2005;30:3320. doi:10.1364/OL.30.003320.

[25] Bartalini S, Cancio P, Giusfredi G, Mazzotti D, De Natale P, Borri S, et al. Frequency-comb-referenced quantum-cascade laser at 4.4 μm. Opt Lett 2007;32:988. doi:10.1364/OL.32.000988.

[26] Gatti D, Gambetta A, Castrillo A, Galzerano G, Laporta P, Gianfrani L, et al. High-precision molecular interrogation by direct referencing of a quantum-cascade-laser to a near-infrared frequency comb. Opt Express 2011;19:17520. doi:10.1364/OE.19.017520.

[27] Peltola J, Vainio M, Fordell T, Hieta T, Merimaa M, Halonen L. Frequency-comb-referenced mid-infrared source for high-precision spectroscopy. Opt Express 2014;22:32429. doi:10.1364/OE.22.032429.

[28] Kovalchuk E V., Schuldt T, Peters A. Combination of a continuous-wave optical parametric oscillator and a femtosecond frequency comb for optical frequency metrology. Opt Lett 2005;30:3141. doi:10.1364/OL.30.003141.

[29] Galli I, Bartalini S, Pastor PC, Cappelli F, Giusfredi G, Mazzotti D, et al. Absolute frequency

measurements of CO_2 transitions at 4.3 μm with a comb-referenced quantum cascade laser. Mol Phys 2013;111:2041–5. doi:10.1080/00268976.2013.782436.

[30] Knabe K, Williams PA, Giorgetta FR, Armacost CM, Crivello S, Radunsky MB, et al. Frequency characterization of a swept- and fixed-wavelength external-cavity quantum cascade laser by use of a frequency comb. Opt Express 2012;20:12432. doi:10.1364/OE.20.012432.

[31] Knabe K, Williams PA, Giorgetta FR, Radunsky MB, Armacost CM, Crivello S, et al. Absolute spectroscopy of N_2O near 4.5 μm with a comb-calibrated, frequency-swept quantum cascade laser spectrometer. Opt Express 2013;21:1020. doi:10.1364/OE.21.001020.

[32] Lamperti M, AlSaif B, Gatti D, Fermann M, Laporta P, Farooq A, et al. Absolute spectroscopy near 7.8 μm with a comb-locked extended-cavity quantum-cascade-laser. Sci Rep 2018;8:1292. doi:10.1038/s41598-018-19188-2.

[33] Phillips CR, Langrock C, Pelc JS, Fejer MM, Jiang J, Fermann ME, et al. Supercontinuum generation in quasi-phase-matched $LiNbO_3$ waveguide pumped by a Tm-doped fiber laser system. Opt Lett 2011;36:3912. doi:10.1364/OL.36.003912.

[34] Mills AA, Gatti D, Jiang J, Mohr C, Mefford W, Gianfrani L, et al. Coherent phase lock of a 9 μm quantum cascade laser to a 2 μm thulium optical frequency comb. Opt Lett 2012;37:4083. doi:10.1364/OL.37.004083.

[35] Toth RA. Frequencies of N_2O in the 1100- to 1440-cm^{-1} region. J Opt Soc Am B 1986;3:1263. doi:10.1364/JOSAB.3.001263.

[36] Perevalov VI, Tashkun SA, Kochanov R V., Liu AW, Campargue A. Global modeling of the $^{14}N_2{}^{16}O$ line positions within the framework of the polyad model of effective Hamiltonian. J Quant Spectrosc Radiat Transf 2012;113:1004–12. doi:10.1016/j.jqsrt.2011.12.008.

[37] Pearson R, Sullivan T, Frenkel L. Microwave spectrum and molecular parameters for $^{14}N_2{}^{16}O$. J Mol Spectrosc 1970;34:440–9. doi:10.1016/0022-2852(70)90025-1.

[38] Andreev BA, Burenin A V., Karyakin EN, Krupnov AF, Shapin SM. Submillimeter wave spectrum and molecular constants of N_2O. J Mol Spectrosc 1976;62:125–48. doi:10.1016/0022-2852(76)90344-1.

[39] Morino I, Fabian M, Takeo H, Yamada KMT. High- J Rotational Transitions of NNO Measured with the NAIR Terahertz Spectrometer. J Mol Spectrosc 1997;185:142–6. doi:10.1006/jmsp.1997.7366.

[40] Drouin BJ, Maiwald FW. Extended THz measurements of nitrous oxide, N_2O. J Mol Spectrosc 2006;236:260–2. doi:10.1016/j.jms.2006.01.005.

[41] Lafferty WJ, Jr. DRL. Rotational constants of excited vibrational states of $^{14}N_2{}^{16}O$. J Mol Spectrosc 1964;14:407–8. doi:10.1016/0022-2852(64)90134-1.

[42] Morino I, Yamada KMT, Maki AG. Terahertz Measurements of Rotational Transitions in Vibrationally Excited States of N_2O. J Mol Spectrosc 1999;196:131–8. doi:10.1006/jmsp.1999.7855.

[43] Pickett HM. Submillimeter, millimeter, and microwave spectral line catalog. Appl Opt 1985;24:2235. doi:10.1364/AO.24.002235.

[44] Toth RA. Linelists of water vapor parameters from 500 to 7500 cm^{-1}. Available via WEB site SISAM.N_2O. 2004. https://mark4sun.jpl.nasa.gov/data/spec/N2O/Readme_N2O.pdf (accessed January 24, 2018).